Effect of Temperature, pH, and Metal Ion Binding on the Secondary Structure of Bacteriorhodopsin: FT-IR Study of the Melting and Premelting Transition Temperatures†

Colin D. Heyes and Mostafa A. El-Sayed*

Laser Dynamics Laboratory, School of Chemistry and Biochemistry, Georgia Institute of Technology, Atlanta, Georgia 30332-0400

Received November 10, 2000; Revised Manuscript Received July 16, 2001

ABSTRACT: We have measured the temperature dependence of the FT-IR spectra of bacteriorhodopsin (bR) as a function of the pH and of the divalent cation regeneration with Ca^{2+} and Mg^{2+}. It has been found that although the irreversible melting transition shows a strong dependence on the pH of the native bR, the premelting reversible transition at 78−80 °C shows very little variation over the pH range studied. It is further shown that the acid blue bR shows a red-shifted amide I spectrum at physiological temperature, which shows a more typical α-helical frequency component at 1652 cm^{-1} and could be the reason for the observed reduction of its melting temperature and lack of an observed premelting transition. Furthermore, the thermal transitions for Ca^{2+}- and Mg^{2+}-regenerated bR (Ca-bR and Mg-bR, respectively) each show a premelting transition at the same 78−80 °C temperature as the native purple membrane, but the irreversible melting transition has a slight dependence on the cation identity. The pH dependence of the Ca^{2+}-regenerated bR is studied, and neither transition varies over the pH range studied. These results are discussed in terms of the cation contribution to the secondary structural stability in bR.

The factors affecting the secondary and tertiary structures of membrane proteins are much less understood than for water-soluble proteins, due to the lipid environment complicating the interpretation of experimental data (*1*, *2*). Bacteriorhodopsin (bR)[1] is one of the most widely studied of the dozen or so membrane proteins whose X-ray structures have been recently determined (*3*−*6*) due to the fact that it is an important biological pump (*7*−*9*) as well as because of its potential applications in biomolecular electronic devices (*10*, *11*). This application comes from its ability to pump protons unidirectionally from the cytoplasmic side of the membrane to the extracellular side. Upon absorption of light, the retinal chromophore, which is bound to the protein through a protonated Schiff base (PSB) at the Lys-216 position, isomerizes from the *all-trans* to the 13-*cis* form. The energy stored at this point drives a series of thermal reactions that result in proton translocation through the membrane by subsequent deprotonation−reprotonation of the Schiff base (SB) linkage (for reviews see refs *12*−*14*). This proton-transfer mechanism does not function if the native bR is deionized by ion exchange or washing with strong acid (*15*−*17*). Upon regeneration with certain cation salts, the proton pumping function is re-formed, but the thermal stability of the purple membrane is only partially regenerated. The extent of this property is dependent on the cation (*18*−*20*).

Calorimetric and spectroscopic studies have shown that there are two main transitions as the temperature of bR is raised (*21*−*23*). There is a small, reversible premelting transition at about 78−80 °C and a major transition at 96 °C, which is irreversible (*24*) and has been assigned to denaturation where the secondary structure shows random coil properties. This can be seen by the appearance of the 1623 cm^{-1} band in the FT-IR spectra (*25*, *26*) as well as other spectroscopic evidence such as X-ray, CD (*27*), and visible absorption (*24*).

The origin of the reversible transition is still not yet unambiguous. It was first measured by Jackson and Sturtevant using DSC and visible absorbance experiments (*24*). It was suggested that the visible absorbance change may be due to a conformational transition affecting the chromophore. They also postulated that the premelting thermal transition at 78 °C might be due to a change in the crystalline packing of the trimers in the lattice. This idea was further examined by X-ray diffraction and CD spectroscopy by Hiraki et al. (*27*). It was found that the diffraction pattern of the purple membrane above 78 °C shows a disordered structure from a breaking of the hexagonal crystal lattice with some local order from the trimer structure in the Bragg peaks and CD spectrum. A similar effect on the X-ray pattern was seen upon removing the cations from bR (*28*).

A number of spectroscopic measurements on the origin of the premelting transition have been carried out. It was found that the amide I peak in the FT-IR spectrum of

† This work was supported by the Chemical Sciences, Geosciences, and Biosciences Division, Office of Basic Energy Science, Office of Sciences, U.S. Department of Energy (under Grant DE-FG02-97ER14799).

* To whom correspondence should be addressed: phone, (404) 894-0292; fax, (404) 894-0294; e-mail, mostafa.el-sayed@chemistry.gatech.edu.

[1] Abbreviations: bR, bacteriorhodopsin; FT-IR, Fourier transform infrared spectroscopy; Ca-bR, calcium(2+)-regenerated bacteriorhodopsin; Mg-bR, magnesium(2+)-regenerated bacteriorhodopsin; DSC, difference scanning calorimetry; CD, circular dichroism; LD, linear dichroism; ED, electron diffraction.

10.1021/bi002594o CCC: $20.00
Published on Web 09/06/2001

bacteriorhodopsin is unusually high, with a value of 1665 cm^{-1} (*29*−*32*). This differs from the usual α-helix frequency of 1652 cm^{-1} (*33*). Krimm and Dwivedi performed normal mode calculations on polyalanine (*34*), which implies the existence of some α_2 helices in bR in which the Φ and Ψ angles are different, resulting in an increase in the H-bond length from 2.86 to 3.00 Å and thus an increase in vibrational frequency by ∼10 cm^{-1}. Various groups have reported data from other techniques that support the existence of α_2 helices such as Raman (*35*), CD (*31*), LD (*32*), and more recently ^{13}C NMR (*36*−*38*).

It must be mentioned, however, that despite all of the spectroscopic evidence, the existence of α_2 helices has not been confirmed in X-ray or electron diffraction structures that have been reported to date (*5*, *39*).

Recently, a time-resolved study of the premelting transformation of bR in D_2O was reported to help to determine the mechanism of melting (*40*). It was found that the amide I band shifts from 1665 to 1652 cm^{-1} within 80 ns, followed by exchange of the amide N−H protons with N−D in >300 ns. The amide I shift is on a fast time scale (<80 ns) and was considered to be too fast to be controlled solely by the solvent effect; however it was not dismissed that this shift may be partially solvent originated. It was also found that the amide I region recovers to the ground state within a few milliseconds as the sample cooled below the pretransition temperature, suggesting the amide I shift to be reversible in this time scale. The amide II N−H and N−D bands did not recover, since the deuteron concentration is greater that the proton concentration in the solvent and the probability of back-exchange is small (i.e., solvent effect is irreversible). More recently, the effect of the protein conformation change in this temperature region on the photocycle has been determined (*41*). It was found that, at temperatures higher than 78 °C but below the main transition, the bR contains a larger proportion of 13-*cis*-retinal and this lowers the photocycle efficiency.

It is not fully known to what extent the cation that is present in bR accounts for the stabilization of the secondary structure. Studies of the thermal denaturation by DSC and CD spectroscopy show strong pH dependence in the native bR, falling to a 65 °C minimum at about pH 2.5 (*19*). It has not yet been investigated if the premelting reversible transition at about 80 °C shows the same pH dependence. Here, we follow the pH dependence of both the premelting transition and the melting transition using FT-IR, which is sensitive to small structural transitions. We also investigate these transitions as a function of the divalent cations Ca^{2+} and Mg^{2+}. Ca^{2+} and Mg^{2+} are known to be present in native bR (*42*) and regenerate the purple color and the proton pumping (for review see ref *20*). However, when these ions are added in excess to deionized bR, the melting temperature does not increase to that of the native bR (*19*, *22*) and varies depending on the cation. Here, we investigate if the protein conformation change is similarly affected by regeneration. We then discuss our findings to help to elucidate potential ion binding sites in native and regenerated bR.

EXPERIMENTAL PROCEDURES

Bacteriorhodopsin (bR) was isolated from *Halobacterium salinarum* by a standard procedure (*43*). The bR was suspended in H_2O and the pH set by addition of HCl or NaOH and measuring on a Beckman pH meter. The solution was left to equilibrate at this pH for several hours and the pH remeasured. By using only strong acid or base, we were able to minimize any ionic strength effects from different buffer solutions. The solutions were centrifuged down to a pellet, and the supernatant was discarded. Resuspension of the bR into D_2O is necessary in order to resolve the amide I and amide II regions of the IR spectrum due to the O−H stretching frequency covering this region. To form a bR pellet in D_2O at each pH, about 5 mL of D_2O (99.9%, Sigma Aldrich) is added the bR·H_2O pellet (about 2 mL), and the excess solvent is allowed to evaporate under argon until a pellet of the same volume is formed. This process is repeated about three to four times to ensure that H_2O is gradually replaced by D_2O, but the concentration of acid or base remains the same as in the original H_2O pellet to ensure the same pD as pH as measured before exchange. Since it is difficult to measure this pD in the pellet, we will refer to the pH as the initial pH before D_2O exchange. During the exchange, the sample is exposed to D_2O for about 24 h, during which time the amide N−H's that are exposed to D_2O are replaced to N−D but the core amide N−H's are not. This pellet is then placed between CaF_2 plates with a 50 μm Teflon spacer and placed in a temperature-controlled sample holder. The FT-IR spectrum is measured on a Bruker IFS-66/S or a Nicolet Magna 860 FT-IR spectrometer as the temperature is increased from 20 to 98 °C. The sample was left to thermally equilibrate at each temperature for 5−10 min before the spectrum is measured. All experiments were repeated three times in order to calculate experimental error in the transition temperatures measured.

The regenerated bR is formed by passing of the native bR through a cation-exchange column filled with ion-exchange resin. $CaCl_2$ (0.01 M) or $MgCl_2$ (0.01 M) is added until a 10:1 molar ratio of cation:bR is reached, where complete regeneration has occurred. The D_2O exchange and spectra measurements are performed as for the native bR.

RESULTS

Figure 1a shows the spectra of native bR at pH 4.4. At this pH, the amide I peak at 1663 cm^{-1} shifts to 1652 cm^{-1} during the reversible transition at about 78 °C. A new band at 1623 cm^{-1} begins to increase in the native bR, corresponding to the melting of the α-helical structure in bR into random conformations. There is a decrease in the amide II N−H peak at 1545 cm^{-1} accompanied by an increase in the peak at 1432 cm^{-1} corresponding to the stretch of the amide II N−D bond. This is more clearly illustrated in Figure 1b, which uses the spectrum at 20 °C as a background, subtracted from each of the higher temperature spectra.

As can be seen in Figure 2a, the FT-IR spectra at pH 2.6, the shift in the amide I peak from 1665 to 1652 cm^{-1} does not occur as it did for the pH 4.4 (and the higher pH samples; data not shown). Instead, the peak at 1665 cm^{-1} just begins to decrease as the peak at 1623 cm^{-1} starts to increase, corresponding to losing α conformation into a random coil-like structure. The decrease of the intensity of the band at 1545 cm^{-1} and the increase of that at 1432 cm^{-1} are observed as the temperature increases. This occurs at a comparable temperature to the melting at about 66 °C. Again, this is more clearly seen in the difference spectra in Figure 2b.

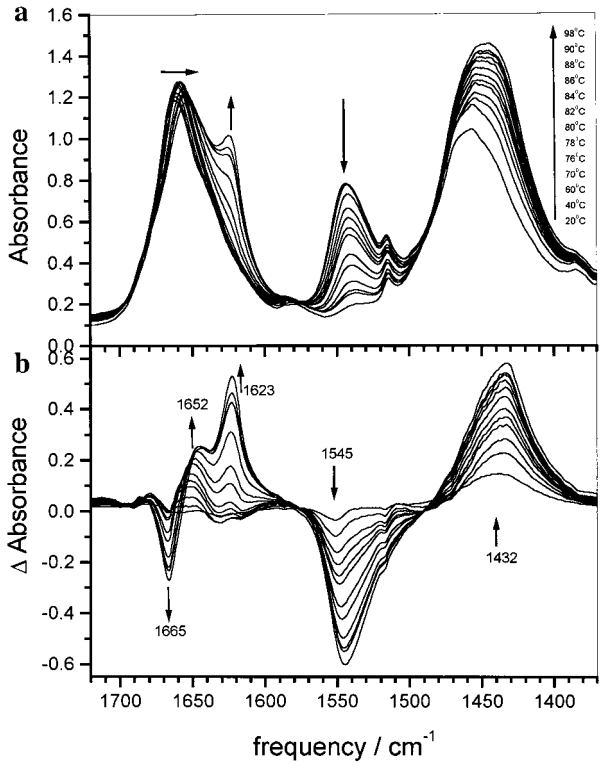

FIGURE 1: (a) FT-IR spectra over the temperature range 20−98 °C for native bR at pH 4.4. It is possible to see the shift in the amide peak at 1665−1652 cm^{-1}. This peak then decreases as the peak at 1623 cm^{-1} increases. Note also the decrease in the peak at 1545 cm^{-1} and the corresponding increase in the peak at 1432 cm^{-1}. (b) Ddifference spectra for bR at pH 4.4 taking the spectra at 20 °C as the background. This allows one to quantify the changes more easily. Positive peaks correspond to the new bands as the temperature increases and negative bands to those that disappear. The peak heights at the maximum are calculated using the Nicolet Omnic software.

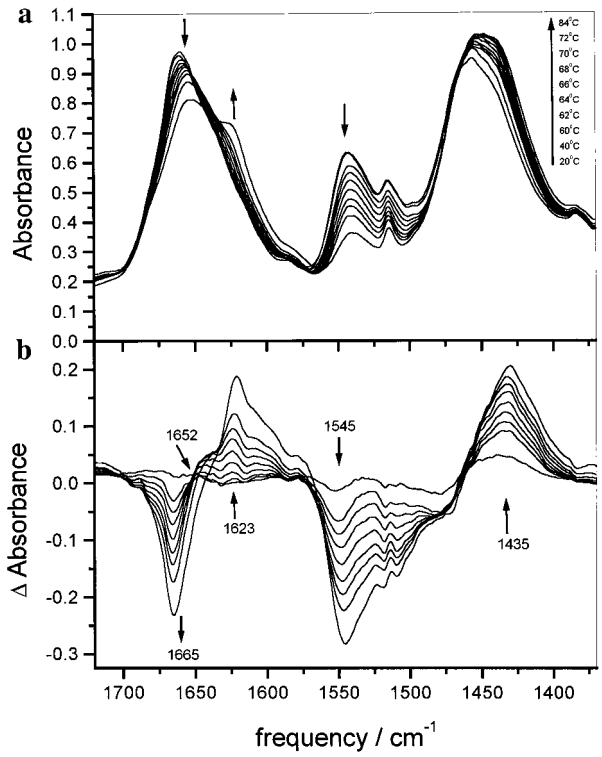

FIGURE 2: (a) FT-IR spectra over the temperature range 20−86 °C for native bR at pH 2.6. The amide peak at 1665 cm^{-1} no longer shifts to 1652 cm^{-1} but just decreases in intensity as the peak at 1623 cm^{-1} increases. Note also the decrease in the peak at 1545 cm^{-1} and the corresponding increase in the peak at 1432 cm^{-1}, which is seen in the pH 4.4 spectra. (b) Difference spectra for bR at pH 2.6 taking the spectra at 20 °C as the background. Again one can see the lack of a peak at 1652 cm^{-1} due to no a_2 to a_1 transition taking place.

To quantify these spectral transitions, the peak height of each peak at the maximum is plotted as a function of temperature for each pH measured. The pH 2.6 sample corresponds to acid blue bR. The peak heights are shown in Figure 3, with each inset corresponding to the first differential of the curves. The first differential allows more sensitive determination of the transition midpoint, which will be a peak rather than just an intensity increase. The melting and premelting transition temperatures are determined from the derivatives of Figure 3b,c (the rise in the 1652 cm^{-1} peak for the premelting transition and the rise in 1623 cm^{-1} for the melting) and plotted as a function of pH. This is illustrated in Figure 4.

From Figure 4, it can be seen that there is a strong pH dependence of the irreversible melting temperature for native bR. This is in agreement with previous calorimetric data, where the melting transition is seen to decrease at lower pH and at higher pH than pH 6.5 (*19*, *21*). Visible absorption and CD data have shown that this major transition is accompanied by the formation of random coil conformation (*21*). The premelting transition in native bR shows very little pH dependence. This smaller thermal transition is not very well quantified using calorimetry due to the lower experimental sensitivity, and CD is not as useful in resolving the small conformational difference that the FT-IR shows in Figure 1. Figure 5 shows that the reversible conformational change also shows very little dependence on the Ca^{2+} or Mg^{2+} cation regeneration, even though the irreversible melting transition temperature is reduced significantly from that observed in native bR. The pH dependence on Ca-bR is also shown in Figure 5, to compare to the native bR. The Ca-bR shows no pH dependence for either transition over the range of pH measured.

The exchange of the protein from H_2O into D_2O allows the exposed, labile amide N−H bonds to be replaced by N−D. The interior N−H amide bonds are not exchanged at low temperature, in agreement with previously reports (*44*, *45*). The peak height of the N−H and N−D bands allows us to determine the extent of deuterium exchange due to exposure of amide N−H to D_2O. These should correspond closely to thermal transitions in which the protein changes conformation exposing new N−H bonds to the D_2O. This can be seen in Figure 3d,e (not all pHs shown for clarity). There is only a slight change until the premelting transition at 78 °C; then the N−D curve begins to increase for all pH values that signals the conformational transition. This continues until the melting temperature is reached, when the increase becomes more pronounced as the unexposed amide bonds exchange the protons for deuterons. This is seen more clearly in the derivative where there is a peak at about the premelting temperature and another at the melting temperature. This feature is more pronounced for some samples than for others but is a reproducible observation. In the inset of Figure 3d, it is possible to resolve two peaks for pH 10.4,

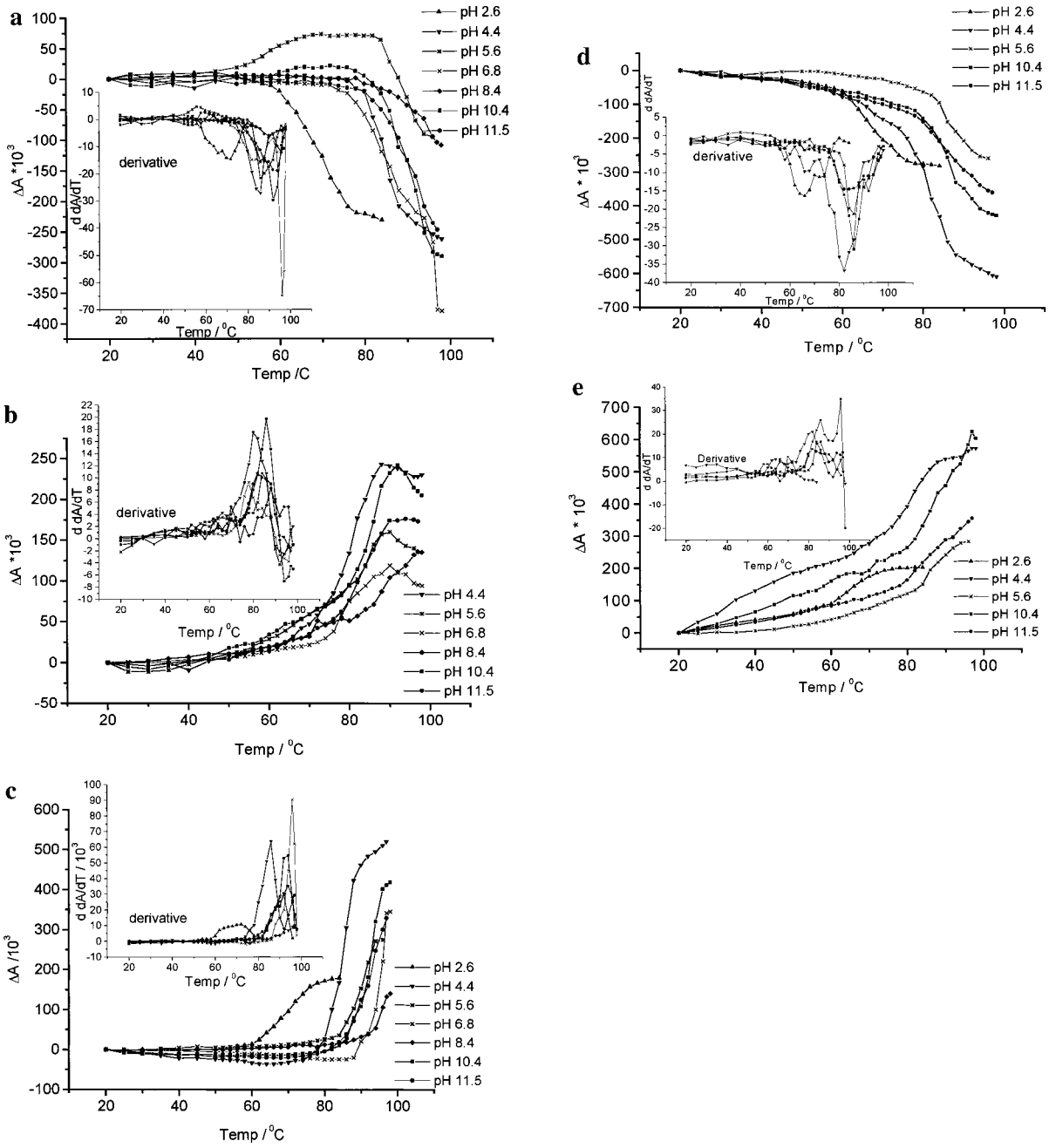

FIGURE 3: Peak heights for the 1665, 1652, 1623, 1545, and 1435 cm^{-1} peaks at each of the temperatures for each pH. The insets for each of these figures are the first derivative of these curves, which show the transition midpoints more clearly.

one at ~80 °C and another at ~93 °C, but for pH 2.6 (acid blue bR, figure 2), there is only one transition at ~63 °C, which corresponds to the lower protein irreversible melting temperature when all the labile amide bonds are exposed to the D_2O. The observation that the slopes of the N−D increase and the N−H decrease in Figure 3d,e are similar but not identical is unexpected. One would expect the exchange to affect the N−H decrease similarly to the N−D increase. This discrepancy may lie in the fact that the peak heights at the maximum were taken at each temperature. There is an obvious difference in the widths of the two amide II bands from Figures 1a and 2a. This indicates that there is some convolution in the regions, possibly from heterogeneity of the sample. However, if the integrals of the peaks were taken, then this would likely cause more interpretation problems than it would solve, since the limits chosen to integrate between are ambiguous and open to controversy. Taking the peak height at the maximum minimizes this ambiguity but does not take account of the heterogeneity.

It was mentioned in the introduction that the solvent may have an effect on the amide I band as well as the amide II band and thus complicate the analysis of the amide I shift. However, comparison of the peak heights of the rise of 1652 cm^{-1} and N−D with temperature (shown normalized to maximum Δ absorbance in order to compare relative slopes for each peak) for pH 4.4 and 10.4 in Figure 6 clearly shows that even though the slopes are about the same at lower temperature possibly due to solvent effect, as the premelting transition temperature is reached, the rise of the 1652 cm^{-1} band is much greater than that of the N−D band. If solvent were to play a large role, then the N−D change would be much greater (since this is the part most affected by solvent)

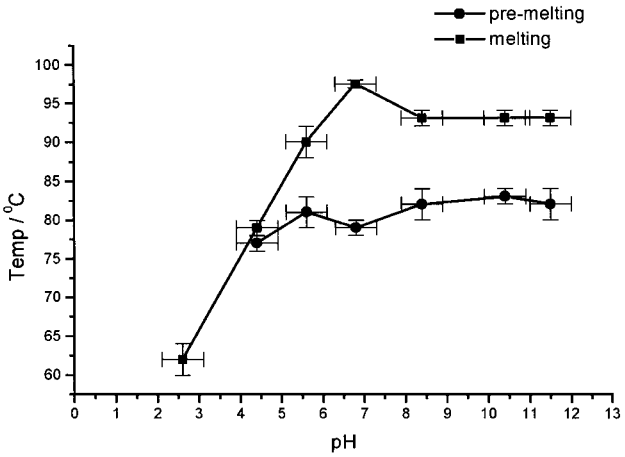

FIGURE 4: Plot of the secondary structure transition temperature as a function of pH for native bR. The melting temperature varies greatly with pH below and above physiological conditions. However, the premelting transition temperature has very little variation for those pH samples that show a premelting transition.

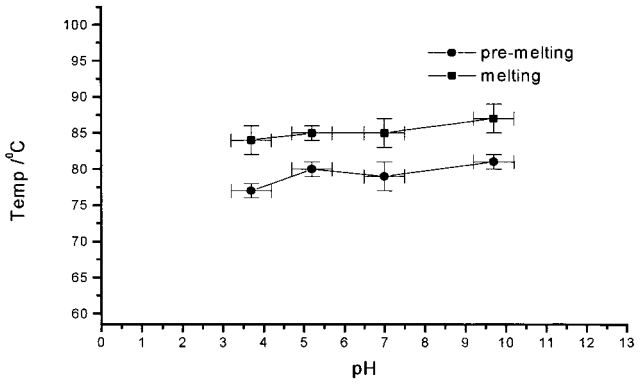

FIGURE 5: Plot of the secondary structure transition temperature as a function of pH for calcium-regenerated bR (Ca-bR). Neither the melting or premelting temperature varies much over the range of pHs measured.

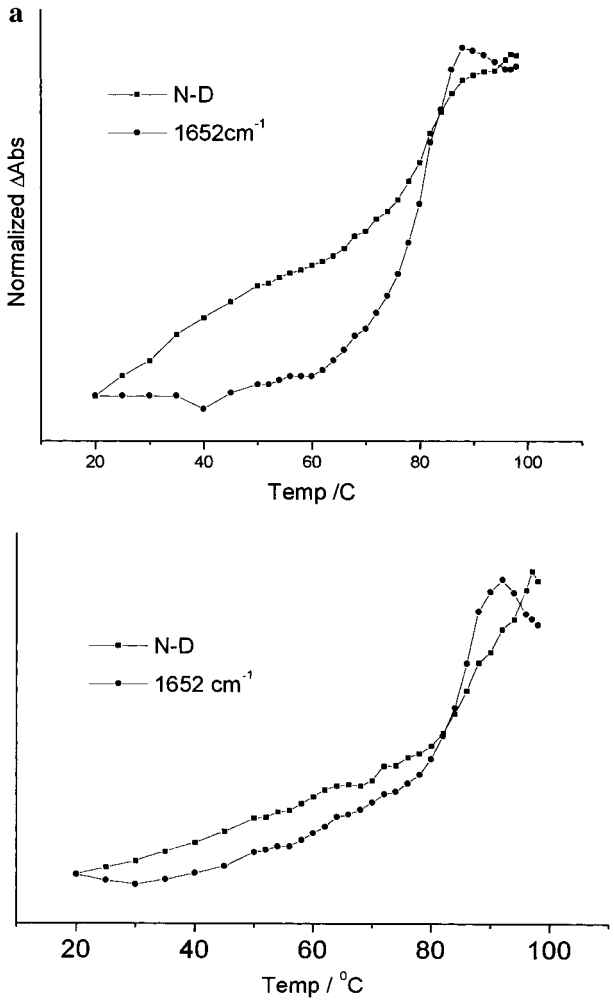

FIGURE 6: Comparison of the peak intensities of the amide I 1652 cm^{-1} and the amide II 1435 cm^{-1} corresponding to N−D for (a) pH 4.4 and (b) pH 10.4. The solvent exchange causes the N−H to become deuterated, but the relative effect on the 1652 cm^{-1} peak is small at low temperatures. The rapid increase of the 1652 cm^{-1} peak compared to the N−D exchange shows that there is a true comformational transition at the premelting transition temperature and not just solvent exchange.

than the 1652 cm^{-1} band or, at most, comparable in change. Since this is clearly not the case, then the 1652 cm^{-1} peak can be assigned to primarily a conformational transition and not just a solvent effect.

To determine the pH effect on the amide I peak at physiological temperature, the amide I band is examined for each pH at 20 °C in Figure 7 as well as for Ca-bR. It can be seen that most of the peaks are very similar, except for the pH 2.6 (i.e., for acid blue bR). At this pH the peak is shifted slightly to the red side, which is the more usual frequency for the α_1 band. Also, the peak is broader, which indicates more heterogeneity in the acid blue membrane. This extends into the 1630 cm^{-1} region, which can be indicative of β-sheet conformations (*46*). This heterogeneity is expected since ion dissociation is not 100% efficient. Therefore, major conformational changes occur upon the formation of the blue membrane even at room temperatures.

To quantify these conformational changes, we have used a peak fitting procedure similar to that of Cladera et al. (*46*). Using the component peaks that they deconvoluted using a number of methods, we have used the program Peakfit, Version 4 (AISN software), to find the relative intensities of the same component bands in our spectrum. This is shown in Figure 8a for pH 8.4 and Figure 8b for pH 2.6, respectively. The other pH values gave bands similar to the one for pH 8.4 as did the Ca- and Mg-regenerated bR (not shown), which is reasonable due to the similarity of the original spectra (Figure 7). One can see that, upon forming blue membrane at pH 2.6, the ratio of the 1667 to 1652 cm^{-1} bands changes considerably, supporting the fact that major conformational changes occur upon deionization of bR. Even though these fitting procedures are not wholly conclusive, the important features seem to show a change in the component bands to favor the more usual 1652 cm^{-1} frequency upon dissociation of the cation.

The results for the transitions at each pH of native bR, of Ca-bR, and of Mg-bR (only at neutral pH) are summarized in Table 1.

DISCUSSION

The thermally induced unfolding of bR in the native state at physiological pH proceeds through a small reversible conformational change at 80 °C. This shifts the vibrational frequency lower by about 10 cm^{-1} (*23*, *40*). Following this transition is the irreversible melting of the protein, in which some of the helical conformations transform to a random

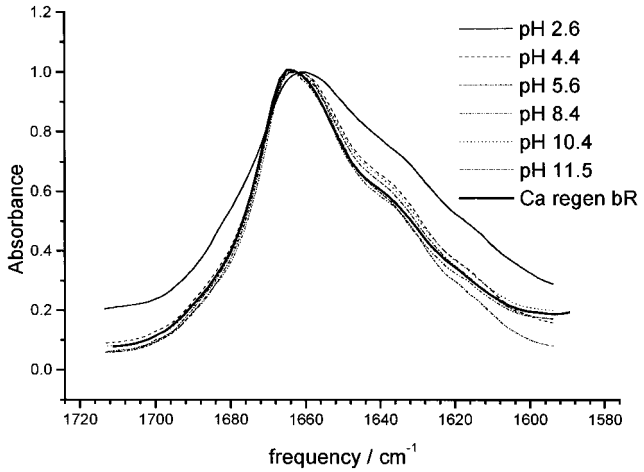

FIGURE 7: Spectra of the amide I peak at 20 °C in native bR at each pH and the Ca-bR at pH 7.0. Each of these peaks shows very similar shape and position with the exception of the acid blue bR, which has a red-shifted and broader peak denoting secondary structure changes in the protein (see text).

conformation. This random form, in which the amide bonds are no longer interacting, has been assigned to a frequency of 1623 cm^{-1} (*23*, *25*, *47*). Understanding the forces that hold together these structures is important to determine the reason membrane proteins are naturally stable over a wide range of conditions. Additionally, it is important to understand the involvement of the cations in the thermal stability, H^+ translocation function, and chromophore absorption energy in bR.

It has been observed that the irreversible melting temperature has a strong dependence on pH, especially as the pH is lowered below 6.5 (*19*). Protonation of some of the negative carboxylic amino acids within the protein occurs as the pH reaches their pK_a values. This changes the hydrophobicity of certain regions of the protein and alters the strength of the cation binding, polar tertiary bonds, and hydrophobic tertiary bonds in both intrahelical and interhelical regions. This accounts for the lowering of the melting temperature with decreasing pH. The dissociation of the cation that causes the observed purple to blue color shift at low pH occurs with an apparent pK_a of about 3.2 (*7*, *48*). It has also been shown by X-ray diffraction and CD spectroscopy (*28*) that the hexagonal crystal lattice is lost, but the trimeric structure is retained upon deionization of the purple membrane. This observation on loss of lattice was disputed by Wakatsuki et al. (*49*). They repeated the experiment as a function of hydration and found that at high hydration the lattice structure is maintained but slightly different to the native, but as the hydration decreases, the lattice structure is lost. This suggests that in Hiraki et al. the sample may be partially dehydrated (*27*). The FT-IR evidence also suggests that deionization also gives rise to a conformational change in the protein. The result is a decrease in the denaturation temperature of the protein to 65 °C. Both of these observations may explain that acid blue bR at pH 2.6 shows no premelting transition (which occurs at 78−80 °C at higher pH).

As was mentioned in the introduction, the X-ray diffraction of native purple membrane above 78 °C is similar to that of the blue membrane studied by Hiraki et al. (*27*). The hexagonal packing is lost but the trimeric structure is retained. The later report (*49*) on maintaining the lattice structure upon deionization has led to an open question on the deionization and sample preparation method effect on the lattice, but in any case, this thermal gel−liquid transition is accompanied by a shift in the amide I peak from 1665 to 1652 cm^{-1}. It is also known that the peak at 1665 cm^{-1} is not present if the native bR is monomerized but is present if the bR is in trimers but not hexagonally packed (*32*, *50*). It was argued by Torres et al. (*32*) that the important condition for the 1665 cm^{-1} band is the interactions between monomers to form of trimers, not on the hexagonal lattice formation, and this stabilizes the α_2 helix. However, we see from Figures 7 and 8 that the 1665 cm^{-1} band for acid blue bR is very much reduced in relation to the band at 1652 cm^{-1} but is present in the cation (Ca^{2+} and Mg^{2+}) regenerated bR. This indicates that the cation is also important for this band and possibly the α_2 helix. It could be that cation binding induces a shift in the α_1 to α_2 equilibrium favoring the α_2 form, which increases the melting temperature and gives rise to a premelting transition from the α_2 to α_1 in native and metal cation regenerated bR at pH >2.6.

The multiple positive charges on the cation have been suggested to bind to more than one carboxylate group within the interior of the protein (*18*, *48*). This has been determined by the observation that several H^+ are exchanged per M^{2+} ion upon binding (*18*). This would account for the increase in interhelical interactions that result in the higher melting temperature for native and regenerated bR. However, the fact that the cation-regenerated bR only partially increases the melting temperature suggests that the cation cannot completely bind the same number of carboxylate groups or, if so, to a lesser binding strength. The fact that the native bR was measured in the absence of any added Ca^{2+} raised the question of ionic effects on the native compared to the regenerated. To check this, the native bR was measured with the addition of 10:1 Ca^{2+} at pH 7. We saw no difference between it and the native bR with no additional Ca^{2+} added (results not shown). The Ca^{2+}-regenerated bR melting temperature shows almost no pH dependence as the native bR did. Therefore, the protonation of some of the carboxylate groups within the protein does not alter the melting temperature. This also suggests that the added cations do not bind to as many carboxylate groups as in the native.

The premelting temperature is unaffected by metal cation regeneration. The Ca-bR and Mg-bR each show a premelting transition at about 78−80 °C, and the Ca-bR shows no pH dependence on this transition. These observations suggest that the amide intrahelical H-bond strengths and angles are not determined by the identity of the cation. However, the FT-IR amide I peak for acid blue native bR is broader and shows more 1652 cm^{-1} character. Therefore, the cation could be partially responsible for the α_2 conformation equilibrium shift, but the temperature at which the transition to α_1 takes place is not cation or pH dependent (above pH 2.6). This suggests that the forces that stabilize the α_2 form depend on the presence of a divalent cation but not on its identity. The reason for this is not completely understood. However, a possible explanation may be that binding of the metal cation to a carboxylate group rearranges part of the protein close to this site into its α_2 form, which allows the trimers to pack into the hexagonal lattice, and may only be reversed upon the removal of the cation or upon heating to 80 °C (i.e.,

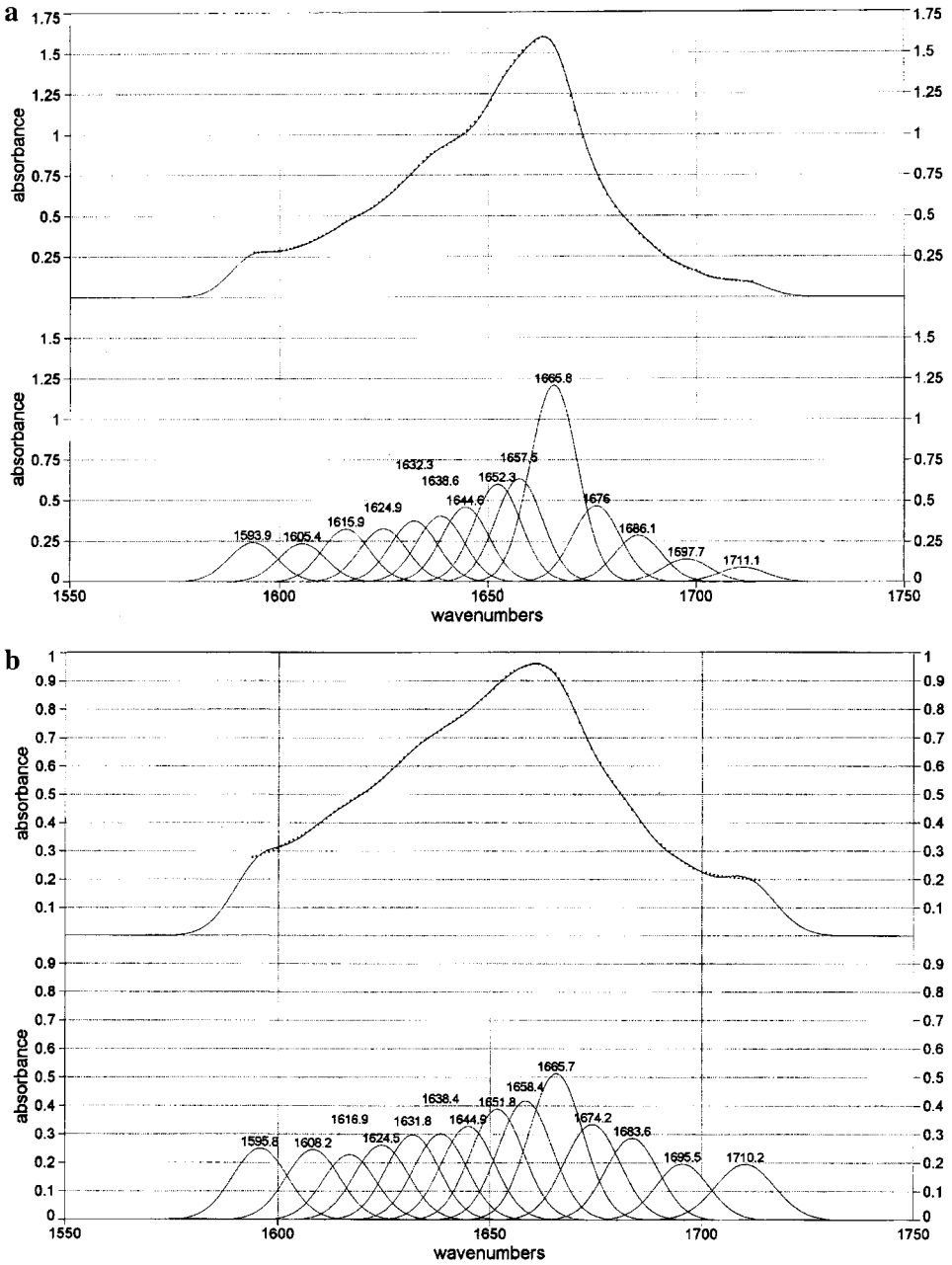

FIGURE 8: Deconvoluted amide I region of native bR at pH 8.4 (a) and pH 2.6 (acid blue) (b). The component bands are as described in ref *46* with the relative intensities varied to fit our data (see text).

remove the cation restraint for α_2 or supply enough thermal energy to overcome this restraint). Once the purple bR is regenerated, any carboxylate groups which are titrated over the pH range from about 4 to 10 have no effect on the secondary structure packing and thus on either of the thermal transitions. This is not true for the native bR. Titration of carboxylate groups of native purple membrane does not affect the reversible premelting transition, but does affect the irreversible melting. Since the interhelical forces are expected to be the major contributions to the melting temperature, this supports the model in which the cation is present inside the protein, binding to more than one carboxylate group in the native bR. The same cannot be concluded for regenerated purple bR. In fact, it is possible that the regenerated purple bR either contains a cation bound to only one carboxylate, or not even inside the protein, but mediates the charge density from the surface, as was proposed by Szundi et al. (*51*). This may explain the large amount of controversy between the specific internal binding model (*18*, *52*−*56*) and the surface-controlled binding model (*51*, *57*−*59*). Most binding experiments have used the assumption that the regenerated purple membrane is color mediated in the same way as the native. These results suggest that is not necessarily the case.

In conclusion, these results have shown that, upon removal of a color-controlling cation by acidification, the protein conformation is changed, which reduces the denaturation temperature to 65 °C. This is below the premelting transition temperature, and therefore such a transition is not observed in acid blue bR. Whether the transition is controlled by this cation directly, or is an implicit thermal property of the protein at 78−80 °C, and the protein melts before this can occur, is not resolved. However, lowering the pH below 7, but keeping it above the blue−purple transition pH has no effect on the α-helical conformation or premelting transition

Table 1: Summary of Thermal Transitions for Native bR and Ca-bR over the pH Ranges Measured, as Well as the Mg-bR at Neutral pH[a]

sample and pH	premelting transition temp/°C	melting transition temp/°C
native, pH 2.6	no transition resolved	62 ± 2
native, pH 4.4	76 ± 1	78 ± 1
native, pH 5.6	78 ± 2	86 ± 2
native, pH 6.8	76 ± 1	96 ± 1
native, pH 8.4	78 ± 2	92 ± 1
native, pH 10.4	79 ± 1	92 ± 1
native, pH 11.5	78 ± 2	92 ± 1
Ca-bR, pH 3.7	76 ± 1	83 ± 2
Ca-bR, pH 5.2	78 ± 1	84 ± 1
Ca-bR, pH 7.0	77 ± 2	84 ± 2
Ca-bR, pH 9.7	78 ± 1	86 ± 2
Mg-bR, pH 7.0	76 ± 2	82 ± 2

[a] The premelting conformation change has little variation in the native and cation-regenerated bR, and no transition was resolved for the acid blue membrane.

temperature. This may be explained by the color-controlling cation affecting the α-helical conformation which in turn allows the lattice to be formed, and it is therefore necessary to transform the helices into α_1 and the noncrystalline phase prior to melting. Furthermore, regeneration with native divalent cations affects the α-helical conformation in the same way, and the transition at 78−80 °C is observed. However, the denaturation temperature for Ca-bR has no pH dependence over the range studied here. Thus, removal of the added cations not in the color-controlling site has no effect on the helical conformation. This observation is consistent with the native bR. However, tertiary interactions that were affected in the native bR upon removal of these cations are not affected in the metal cation regenerated bR. Since the melting temperature is not fully restored, it seems natural to conclude that these tertiary interactions are not fully restored upon cation regeneration.

Whether the existence of α_2 helices is confirmed or not, it is clear that a cation, which is likely in the color-controlling site, is necessary to stabilize the forces that allow packing of the lattice, and this in turn affects the amide I frequency and the helix. The electron diffraction model proposed by Henderson et al. (*60*) and refined by Grigorieff et al. (*39*) does not show the α_2 helical angles. It must be considered a possibility that, upon crystallization for ED or X-ray, one may lose or move the cation (which also has not been seen), and the helices may transform into α_1 as in the deionized bR. Preparation of the crystals involves a lengthy procedure in which lipids are removed and subsequently replaced under nonphysiological conditions. This undoubtedly has an impact on the protein secondary structure and possibly the cation binding. The model proposed by Grigorieff et al. (*39*) also shows the degree of order throughout the protein, of which the highest order is in the retinal pocket, close to the Asp groups that are thought of as the counterions for the cation, and may suggest that this is where the forces that crystallize the protein originate. Whether or not the cation is present in their final crystal, using this model together with our results, one may speculate that if the forces that stabilize α_2 and the lattice packing are due to the cation, as proposed earlier, this lends support to the specific internal binding of the cation in the native bR.

ACKNOWLEDGMENT

The authors acknowledge Dr. Jianping Wang for technical help and useful discussions. The authors also express their acknowledgment to a conscientious reviewer that has participated in useful discussions on the paper.

REFERENCES

1. White, S. H. (1994) *Membrane Protein Structure: Experimental Approaches*, Oxford University Press, New York.
2. White, S. H., Wimley, W. C., Ladokhin, A. S., and Hristova, K. (1998) *Methods Enzymol. 295*, 62−87.
3. Luecke, H., Richter, H.-T., and Lanyi, J. K. (1998) *Science 280*, 1934−1937.
4. Leuke, H., Schobert, B., Richter, H. T., Cartailler, J. P., and Lanyi, J. K. (1999) *Science 286*, 255−260.
5. Leuke, H., Schobert, B., Richter, H. T., Cartailler, J. P., and Lanyi, J. K. (1999) *J. Mol. Biol. 291*, 899−911.
6. Sass, H. J., Buidt, G., Gessenich, R., Hehn, D., Neff, D., Schlesinger, R., Berendzen, J., and Ormos, P. (2000) *Nature 406*, 649−653.
7. Oesterhelt, D., and Stoeckenius, W. (1971) *Nat. New Biol. (London) 233*, 149−152.
8. Oesterhelt, D. (1974) *Membrane Proteins Transport and Phosphorylation* (Azzone, G. F., Klingenberg, M. E., and Quagliariello, E., Eds.) pp 79−84, North-Holland, Amsterdam, The Netherlands.
9. Kayushin, L. P., and Skulachev, V. P. (1974) *FEBS Lett. 39*, 39−42.
10. Birge, R. R., Gillespie, N. B., Izaguirre, E. W., et al. (1999) *J. Phys. Chem. B 103*, 10746−10766.
11. Hampp, N. (2000) *Chem. Rev. 100*, 1755−1776.
12. Mathies, R. A., Lin, S. W., Ames, J. B., and Pollard, W. T. (1991) *Annu. Rev. Biophys. Biophys. Chem. 20*, 491−518.
13. Lanyi, J. K. (1993) *Biochim. Biophys. Acta 1183*, 241−261.
14. Lanyi, J. K. (1999) *FEBS Lett. 464*, 103−107.
15. Kimura, Y., Ikegami, A., and Stoeckenius, W. (1984) *Photochem. Photobiol. 40*, 641−646.
16. Mowery, P. C., Lozier, R. H., Chae, Q., Tseng, Y.-W., Taylor, M., and Stoeckenius, W. (1979) *Biochemistry 18*, 4100−4107.
17. Chang, C. H., Chen, J. G., Govindjee, R., and Ebrey, T. (1985) *Proc. Natl. Acad. Sci. U.S.A. 82*, 396−400.
18. Ariki, M., and Lanyi, J. K. (1986) *J. Biol. Chem. 261*, 8167−8174.
19. Kresheck, G. C., Lin, C. T., Williamson, L. N., Mason, W. R., Jang, D. J., and El-Sayed, M. A. (1990) *J. Photochem. Photobiol., B 7*, 289−302.
20. El-Sayed, M. A., Yang, D., Yoo, S.-K., and Zhang, N. (1995) *Isr. J. Chem. 35*, 465−474.
21. Brouillette, C. G., Muccio, D. D., and Finney, T. K. (1987) *Biochemistry 26*, 7431−7438.
22. Cladera, J., Galisteo, M. L., Dunach, M., Mateo, P. L., and Padros, E. (1988) *Biochim. Biophys. Acta 943*, 148−156.
23. Taneva, S. G., Caaveiro, J. M. M., Muga, A., and Coni, F. M. (1995) *FEBS Lett. 367*, 297−300.
24. Jackson, M. B., and Sturtevant, J. M. (1978) *Biochemistry 17*, 911−915.
25. Arrondo, J. R., Castresana, J. M., Valpuesta, J. M., and Goni, F. M. (1994) *Biochemistry 33*, 11650−11655.
26. Muga, A., Arrondo, J. L. R., Bellon, T., Sancho, J., and Bernabeu, C. (1993) *Arch. Biochem. Biophys. 300*, 451−457.
27. Hiraki, K., Hamanaka, T., Mitsui, T., and Kito, Y. (1981) *Biochim. Biophys. Acta 647*, 18−28.
28. Heyn, M. P., Dudda, C., Otto, H., Seiff, F., and Wallat, I. (1989) *Biochemistry 28*, 9166−9172.
29. Rothschild, K. J., and Clark, N. A. (1979) *Biophys. J. 25*, 473−487.
30. Rothschild, K. J., and Clark, N. A. (1979) *Science 204*, 311−312.
31. Gibson, N. J., and Cassim, J. Y. (1989) *Biochemistry 28*, 2134−2139.
32. Torres, J., Sepulcre, F., and Padros, E. (1995) *Biochemistry 34*, 16320−16326.

33. Fraser, R. D. B., and MacRae, T. P. (1973) *Conformation in fibrous proteins and related synthetic polypeptides*, Academic Press, New York.
34. Krimm, S., and Dwivedi, A. M. (1982) *Science 216*, 407−408.
35. Vogel, H., and Gaertner, W. (1987) *J. Biol. Chem. 262*, 11464−11469.
36. Tuzi, S., Naito, A., and Saito, H. (1994) *Biochemistry 33*, 15046−15052.
37. Tuzi, S., Naito, A., and Saito, H. (1996) *Eur. J. Biochem. 239*, 294−301.
38. Kawase, Y., Tanio, M., Kira, A., Yamaguchi, S., Tuzi, S., Naito, A., Kataoka, M., Lanyi, J. K., Needleman, R., and Saito, A. (2000) *Biochemistry 39*, 14472−14480.
39. Grigorieff, N., Ceska, T. A., Downing, K. H., Baldwin, J. M., and Henderson, R. (1996) *J. Mol. Biol. 259*, 393−421.
40. Wang, J., and El-Sayed, M. A. (1999) *Biophys. J. 76*, 2777−2783.
41. Wang, J., and El-Sayed, M. A. (2000) *Biophys. J. 78*, 2031−2036.
42. Griffiths, J. A., King, J., Browner, R., and El-Sayed, M. A. (1996) *J. Phys. Chem. 100*, 929−933.
43. Oesterhelt, D., and Stoeckenius, W. (1974) *Methods Enzymol. 31*, 667−678.
44. Earnest, T. N., Roepe, P., Braiman, M. S., Gillespie, J., and Rothschild, K. J. (1986) *Biochemistry 25*, 7793−7798.
45. Kluge, T., Olejnik, J., Smilowitz, L., and Rothschild, K. J. (1998) *Biochemistry 37*, 10279−10285.
46. Cladera, J., Sabes, M., and Padros, E. (1992) *Biochemistry 31*, 12363−12368.
47. Cladera, J., Galisteo, M. L., Sabes, M., Mateo, P. L., and Padros, E. (1992) *Eur. J. Biochem. 207*, 581−585.
48. Jonas, R., Koutalos, Y., and Ebrey, T. G. (1990) *Photochem. Photobiol. 52*, 1163−1177.
49. Wakatsuki, S., Kimura, Y., Stoeckenius, W., Gillis, N., Eliezer, D., Hodgson, K. O., and Doniach, S. (1994) *Biochim. Biophys. Acta 1185*, 160−166.
50. Popot, J. L., Gerchman, S. E., and Engelman, D. M. (1987) *J. Mol. Biol. 198*, 655−676.
51. Szundi, I., and Stoeckenius, W. (1989) *Biophys. J. 56*, 369−383.
52. Jonas, R., and Ebrey, T. G. (1991) *Proc. Natl. Acad. Sci. U.S.A. 88*, 149−153.
53. Zhang, Y. N., Sweetman, L. L., Awad, E. S., and El-Sayed, M. A. (1992) *Biophys. J. 61*, 1201−1206.
54. Zhang, N. Y., and El-Sayed, M. A. (1993) *Biochemistry 32*, 14173−14175.
55. Yoo, S.-K., Awad, E. S., and El-Sayed, M. A. (1995) *J. Phys. Chem. 99*, 11600−11604.
56. Stuart, J. A., Vought, B. W., Zhang, C.-F., and Birge, R. R. (1995) *Biospectroscopy 1*, 9−28.
57. Szundi, I., and Stoeckenius, W. (1987) *Proc. Natl. Acad. Sci. U.S.A. 84*, 3681−3684.
58. Szundi, I., and Stoeckenius, W. (1988) *Biophys. J. 54*, 227−232.
59. Varo, G., Brown, L. S., Needleman, R., and Lanyi, J. K. (1999) *Biophys. J. 76*, 3219−3226.
60. Henderson, R., Baldwin, J. M., Ceska, T. A., Zemlin, F., Beckmann, E., and Downing, K. H. (1990) *J. Mol. Biol. 213*, 899−929.

BI002594O